Catalytic Performance and Nanoclay Effects on Post-Solid-State Polyamidation: The Case of Polyamide 6,6 Nanocomposites

A. C. Boussia, M. O. Konstantakopoulou, S. N. Vouyiouka, C. D. Papaspyrides

Laboratory of Polymer Technology, School of Chemical Engineering, National Technical University of Athens, Zographou Campus, Athens 15780, Greece

ABSTRACT: The catalytic performance of common additives was explored during the solid-state postpolymerization (SSP) of polyamide 6,6 prepolymers. In particular, the influence of a phosphorous-containing antioxidant and its combination with a nanofiller (clay) was examined during the SSP reaction at 200°C for times up to 4 h. The antioxidant, at a concentration of 1 phr, was found to strongly accelerate the SSP process by more than quintupling (435%) the reaction rate. The antioxidant–clay system (1 phr each) also catalyzed the SSP process and resulted in a near tripling (197%) of the reaction rate; this implied, however, a reduced single antioxidant catalytic performance. The latter was attributed to counteractions involving the diffusivity of polycondensation water versus clay hydrophilicity and to physical adsorption phenomena between the antioxidant and the clay. © 2012 Wiley Periodicals, Inc. J Appl Polym Sci 125: E320–E326, 2012

Key words: catalysts; clay; nanocomposites; polyamides; solid-state polymerization

INTRODUCTION

Polyamides (PAs) and polyesters are commercially important condensation polymers with a broad field of applications, including films, bottles, fibers, and shaped engineering parts. They are conventionally produced by solution and/or melt polymerization techniques, which, however, stop at a low- or medium-molecular-weight products because of problems arising from severe increases in the melt viscosity and operating temperatures.[1] Solid-state postpolymerization (SSP) comes as an answer when higher molecular weight requirements arise, as in the case for injection- and stretch-blow-molding applications. It involves the heating of the starting material in an inert atmosphere or *in vacuo* at a temperature higher than the glass-transition temperature but lower than the onset of melting [melting temperature (T_m)]. SSP is applied extensively on an industrial scale as a finishing stage (post SSP) because of the easy material handling, the low extent of product degradation, and the plain equipment requirement.[2,3]

SSP constitutes a complex process because it involves chemical and physical stages. The possible rate-limiting steps can be determined on the basis of the reversible reaction and the solid nature restrictions, being chemical reaction, segmental diffusion in the amorphous phase and condensate removal.[2,3] Several variables may engage with the rate-limiting steps, such as the reaction temperature, prepolymer molecular weight, crystallinity, crystal morphology, and reacting particle geometry. Moreover, the incorporation of additives, such as catalysts (metals, acids, bases), reactive additives (chain extenders, branching agents), and inert ones, is found to strongly influence the SSP processes.[4]

In particular, catalysis in SSP processes constitutes a significant research area to overcome the main industrial SSP drawbacks, including its low rate compared to the melt technique and sintering problems.[4] A number of basic, acidic, or neutral compounds, such as H_3PO_4, H_3BO_3, H_2SO_4, $ZnCl_2$, and MgO, are found to speed up the monomer SSP process.[4–7] The relevant catalysis mechanism in the case of acid-catalyzed polyamidation involves the addition of a proton from the strong acid to the carbonyl oxygen; this renders it more susceptible to the nucleophilic attack by NH_2.[8–11]

With a focus on polyamide 6,6 (PA 6,6) prepolymer SSP, mainly phosphorus (P)-based compounds are used as catalysts, such as 2-(2′-pyridyl) ethyl phosphonic acid, sodium hypophosphite (SHP), and manganese hypophosphite.[4,11–13] More recently, the catalytic effect of sterically hindered hydroxyphenylalkylphosphonic ester and monoester salts has been proven.[14,15] The catalysis was related to the structure of the phosphonate and the additive mobility,

Correspondence to: C. D. Papaspyrides (kp@softlab.ece.ntua.gr).

whereas partial incorporation in the polymer chain was assumed, as the catalyst efficiency was even more pronounced when added during synthesis of the PA 6,6 salt.[14] Triphosphite esters, such as triarylphosphites, have also been reported as SSP catalysts, but the relevant literature is restricted and patented.[14,16] On the other hand, during solution and/or melt polycondensation, triarylphosphite condensing action has been shown by several groups,[17–23] mainly for the formation of aromatic PAs in solution at moderate temperatures. As an example, Aharoni and coworkers[21–23] studied polyamidation in the presence of triarylphosphites in solution[22] and in the melt state during extrusion.[21] They suggested that triarylphosphites serve as chain extenders for the polyamidation reaction.

Another additive family that has lately been used extensively for the modification and/or improvement of material properties is that of nanoparticles, such as silica, carbon nanotubes, and clays.[24–27] A key feature of these nanosized additives is their recently reported catalytic action during SSP.[28–32] Particularly for PA 6,6 SSP, the catalyzing effect of clay was observed, quantified, and interpreted for the first time in our recent work;[32] this, thus, promoted nanofiller incorporation not only for the modification and/or improvement of material properties but also for their performance as SSP multifunctional catalysts.

This study constituted, in fact, a continuation of our previous study[32] in catalyzed PA 6,6 SSP processes through the exploration of the joint catalytic performance of a nanoclay and a phosphorous-containing antioxidant. This is of great importance because it is possible to provide a suitable SSP catalyst system through the combination of the benefits of catalysis, thermal stability, and nanotechnology. In particular, the selected organoclay has already been proven to catalyze PA 6,6 SSP[32] and to tailor polymer characteristics. On the other hand, the selected commercial phosphorous-containing antioxidant product is used to stabilize PA molded parts, fibers, and films and provides very good processing and long-term thermal stability.

EXPERIMENTAL

Starting materials

The PA 6,6 resin (Terez) was supplied by TerHell Plastic GmbH (Herne, Germany). The antioxidant Irganox B1171 (Fig. 1) was supplied by Ciba Lampertheim GmbH (Lampertheim, Germany), and it was a 1 : 1 blend of a sterically hindered phenolic amide {*n,n'*-hexane-1,6-diylbis[3-(3,5-di-*tert*-butyl-4-hydroxy-phenylpropionamide], Fig. 1(a)} and a phosphite [tris(2,4-di-*tert*-butylphenyl)phosphite, Fig. 1(b)]. The
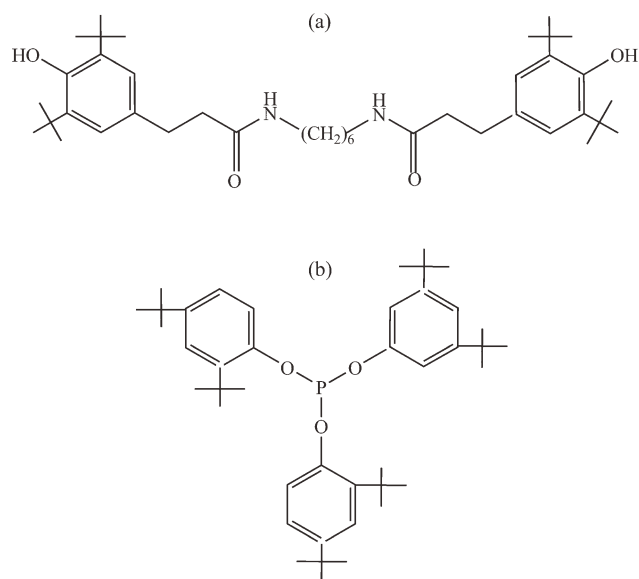

Figure 1 Chemical composition of antioxidant Irganox B1171. It is a 1 : 1 blend of (a) Irganox 1098 and (b) Irgafos 168.

organoclay used was based on natural montmorillonite of 1.15 mequiv/g cation-exchange capacity, modified with octadecylbenzyldimethylammonium chloride at an extent of 100% cation-exchange capacity (S&B Industrial Minerals SA, Athens, Greece). Additive incorporation was achieved through melt intercalation in a twin-screw corotating intermeshing extruder (Thermo Fisher Scientific, Inc., temperature = 255–290°C, screw speed (ω) = 300 rpm, *in vacuo*). Virgin PA 6,6 was also extruded under identical conditions for comparison reasons. Before any SSP runs, all prepolymers were sieved, the particle size range selected was 1.14–1.70 mm, and the samples were dried *in vacuo* (80°C, 4 h). The characteristics of the prepolymers are presented in Table I.

Solid-state polymerization

A fixed-bed, bench-scale reactor assembled by INVISTA Co., Inc. (Experimental Station, Wilmington, DE) and set up in our laboratory in Athens, Greece, was used to solid-state polymerize the prepolymers under the conditions presented in Table I. A detailed description of the reactor can be found in a previous publications of ours.[15,32–34]

Characterization

Wide-angle X-ray diffraction

The achieved PA 6,6 nanocomposites structure was confirmed by wide-angle X-ray diffraction analysis in the range 2–10° (2θ). Spectra were collected from a Siemens powder D-5000 diffractometer equipped with Cu Kα$_1$ radiation (λ = 1.5405 Å) and operating

TABLE I
Characteristics of the Prepolymers and SSP Experimental Conditions

	Characterization of the modified prepolymers			
	M_n (g/mol)	T_m (°C)	X_c (%)	T_c (°C)
PA 6.6 (PA0)	14,200	267.7 ± 0.0	38.2 ± 1.6	238.4 ± 0.1
PA 6.6 + 1 phr Irganox B1171 (PA1)	17,200	267.1 ± 0.0	37.5 ± 0.0	237.3 ± 0.0
PA 6.6 + 1 phr clay (N-PA0)	14,000	267.4 ± 0.1	34.3 ± 0.7	239.9 ± 0.1
PA 6.6 + 1 phr Irganox B1171 + 1 phr clay (N-PA1)	16,900	266.4 ± 0.0	37.7 ± 0.0	239.0 ± 0.0

	SSP conditions		
	Temperature (°C)	Time (h)	Inert gas
PA0	200	0, 1, 2, 4	N_2 (260 mL/min)
PA1	200	0, 1, 2, 4	N_2 (260 mL/min)
N-PA0	200	0, 1, 2, 4	N_2 (260 mL/min)
N-PA1	200	0, 1, 2, 4	N_2 (260 mL/min)

at 40 kV and 30 mA. Measurements were performed on thermoformed 20 μm thick films.

Differential scanning calorimetry (DSC)

The thermal characteristics of the prepolymers were determined with a PerkinElmer Pyris 6 DSC instrument (Waltham, MA). For each measurement, a sample (≈10 mg) was heated to 300°C at 10°C/min under flowing nitrogen, and it remained at this temperature for 10 min to erase its thermal history. Then, it was cooled to 30°C at the same rate. During heating, T_m and the enthalpy of fusion (ΔH_m) were obtained, whereas from the cooling scan, the crystallization temperature (T_c) was recorded. The deviation of the mean values was derived through duplicate measurements. The degree of mass fraction crystallinity (X_c) was calculated from Eq. (1):

$$X_c(\%) = \Delta H_m / \Delta H_0 (1 - \varphi) \quad (1)$$

where φ is the nanoclay and/or antioxidant content and ΔH_0 is the enthalpy of fusion of 100% crystalline PA 6,6 (50.45 cal/g).[35]

End-group analysis

In all PA grades, the end-group content was determined by potentiometric titration, as previously described.[34] The number-average molecular weight (M_n; g/mol) was calculated as follows [Eq. (2)]:[36]

$$M_n = \frac{2 \times 10^6}{[NH_2] + [COOH]} \quad (2)$$

where $[NH_2]$ and $[COOH]$ are the amine and carboxyl group concentrations (mequiv/kg), respectively. The deviations of the mean values were derived through duplicate measurements.

Theoretical: Modeling of SSP kinetics

The SSP kinetics were studied with a simple third-order Flory theory-based model [Eq. (3)], with only the polycondensation reaction considered because of the low reaction temperature applied in conjunction with the constant byproduct removal through convection by flowing nitrogen. The pertinent rate expression was found to fit the end group-based SSP data very well and to describe the overall process on the basis of our previous publications.[3,32,34] This simple kinetic model led to values of the apparent rate constants at any given reaction time; a mean value was determined, and the standard deviation of the mean was calculated, indicating the model effectiveness for PA 6.6 and modified grades:

$$k_3 t = \frac{1}{D_0^2} \ln \frac{[COOH]_0 - [NH_2]_0 p_t}{[COOH]_0 (1 - p_t)}$$
$$- \frac{1}{D_0} \left(\frac{1}{[COOH]_0 - [NH_2]_0 p_t} - \frac{1}{[COOH]_0} \right) \quad (3)$$

where $[COOH]_0$ and $[NH_2]_0$ are the initial concentrations of the carboxyl and amine groups (mequiv/kg), respectively, D_0 is the initial carboxyl group excess (mequiv/kg), p_t is the polymerization conversion at any given reaction time, and k_3 is the apparent SSP rate constant for third-order kinetics (kg^2 mequiv^{-2} h^{-1}).

A special characteristic of SSP kinetics is that as SSP proceeds, a large part of the reactive groups disappears and the concentration of the residual reactive moieties in the amorphous regions decreases. The reaction rate becomes dependent more and more on the segmental diffusion, and the kinetic constants are expected to decrease progressively as far as the closest end-group pairs have reacted; this implies the dependence of the rate constant on SSP time.[2,3]
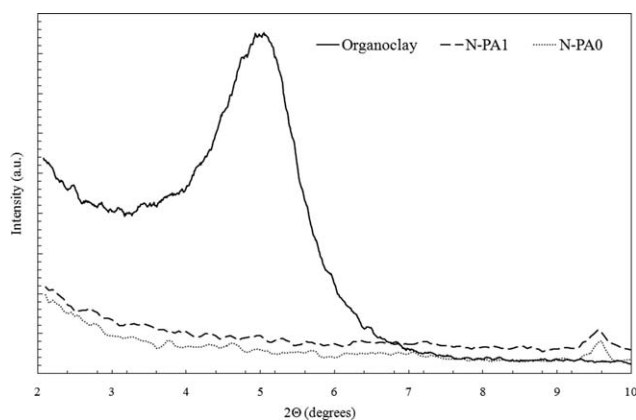
Figure 2 XRD spectra of the PA 6,6 nanocomposite prepolymers N-PA0 and N-PA1.

RESULTS AND DISCUSSION

Prepolymer modification

The incorporation of the examined catalyst systems was performed through twin-screw extrusion. On the basis of a previous patent by our group on PA 6,6 SSP,[14] the *in situ* incorporation of the phosphorous-containing antioxidant during PA synthesis would potentially result in a stronger catalytic performance. However, such an incorporation technique in the nanocomposites case would result in poor nanoclay dispersion:[37] it was found that during the *in situ* intercalative polymerization of the PA 6,6–clay nanocomposites, a competitive ion exchange between the diamine component of the PA salt and the organoclay alkylammonium surfactant took place. This led to clay interlayer collapse due to bridging and restricted the potential for fully exfoliated nanocomposite structures. Therefore, on the basis of these previous findings, the melt intercalation technique was herewith applied for the additive incorporation. This led to exfoliated nanocomposite structures, as evidenced in Figure 2, where the organoclay characteristic peak disappeared, regardless of the antioxidant component presence.

The prepolymer molecular weight analysis is presented in Table I, where it is shown that all grades were of similar M_n and were suitable for subsequent SSP.[2,3] In addition, there was no evidence of organoclay surfactant thermal degradation, which could subsequently lead to PA matrix degradation during extrusion,[24,25] because the nanocomposite matrices' molecular weights were not reduced. Meanwhile, there was an absence of yellowing and/or insoluble fractions during analyses, which are typical indications of branching reactions.[32] However, it should be mentioned that the grades containing 1 phr antioxidant (PA1 and N-PA1) exhibited higher molecular weights compared to PA0 and N-PA0; this implied

the occurrence of a higher polymerization extent already during the applied extrusion step.

With regard to the thermal characteristics of the prepolymers, no significant variation in the T_m or X_c values was observed; this allowed us to compare these materials during subsequent SSP runs.[2,3] On the other hand, the T_c values of the nanocomposite grades N-PA0 and N-PA1 appeared to be slightly higher than those of PA0 and PA1; this is a typical indication of a clay heterogeneous nucleation effect.[24,25,32]

Catalytic performance of the phosphorous-containing antioxidant

The molecular weight evolution of PA 6,6 containing 1 phr antioxidant (PA1) revealed the strong catalyzing action of the phosphorous additive during SSP at 200°C [Fig. 3(a)]; this led to an SSP product of $M_n = 37,300$ g/mol (vs 21,800 g/mol of PA0). The mean rate constant ($1000k_3$) also expressed the observed acceleration because it was found 435% higher for PA1 than for PA0 (Fig. 4). This enhanced PA1 rate constant prevailed all through the course of the SSP process (Fig. 5). In particular, the PA1
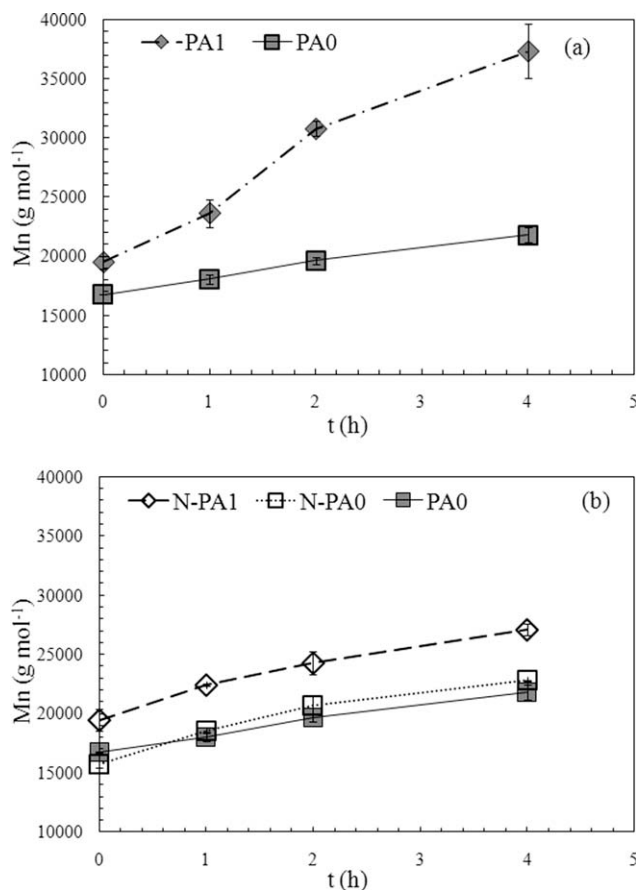

Figure 3 Evolution of M_n during SSP at 200°C of (a) PA1 versus PA0 and (b) N-PA1 versus N-PA0 and PA0.
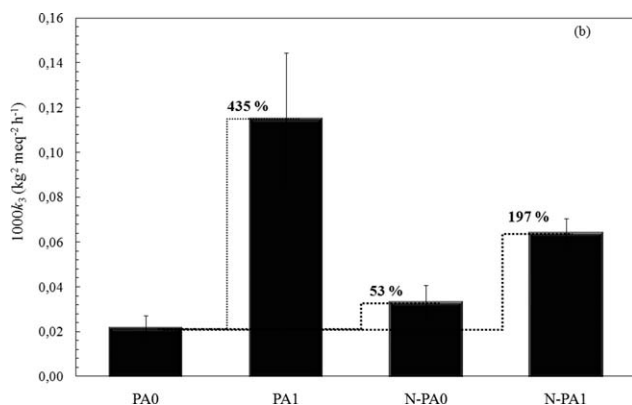
Figure 4 Reaction rate constants ($1000k_3$) of SSP at 200°C for the PA0, PA1, N-PA0, and N-PA1 grades.

rate constant was found to increase from the very beginning of the reaction (1 h) compared to PA0; this showed the readily activated catalyzing power of the antioxidant. At the end of SSP, PA1 also presented a high reaction rate, unlike typical SSP kinetic development,[3] which is characterized by lower final rates because of end group deactivation by diffusion limitation emergence. The latter indicated the immunity of the catalyzed system to such limitations and implied that the phosphorus additive seemed to promote both chemical reaction and the diffusion of end groups.

On the basis of the literature and as already discussed in the Introduction, the catalytic action of the tested antioxidant was attributed to its triphenylphosphite constituent.[14,16–23] Furthermore, our experimental data indicated a considerable molecular weight increase during extrusion in the presence of the antioxidant (Table I, PA1 vs PA0 and N-PA1 vs N-PA0). In other words, it seemed that this strong catalyzing action was readily activated already from the extrusion step.

Catalytic performance of the antioxidant–clay system

On the basis of the molecular weight evolution during SSP [Fig. 3(b)], the antioxidant–clay system (N-PA1) was proven to be beneficial for PA 6,6 SSP and to ensure a constant molecular weight increase and a higher final value (M_n = 27,100 vs 21,800 g/mol for PA0). This enhancement was expressed by a 197% rate constant ($1000k_3$) increase in the presence of the dual-catalyst system (Fig. 4). Meanwhile, this combination of antioxidant and clay (N-PA1) exceeded the single-clay (N-PA0) catalyst efficiency by 144%. However, this system performance was not superior to the catalytic action of antioxidant alone and implied significant counteraction effects between the antioxidant and clay on the SSP rate (Fig. 4).

Role of the polycondensation water

To interpret this reduction of antioxidant catalyzing potential in the presence of the nanofiller, a fundamental characteristic of organoclays should be considered. In particular, although organoclays are conventionally considered hydrophobic because of the addition of alkylammonium cations, some hydrophilicity persists even after their organophilization treatment. Indeed, it was noted that whereas pristine clays can absorb up to seven times their weight in water, organoclays can absorb up to 5–10% of their weight, which is not, however, a negligible amount at all.[38] More specifically, water absorption still occurs on the exterior of clay aggregates and along the hydrophilic layer edges and depends on the environmental conditions, such as relative humidity.[39]

In this direction, when one considers the favorable conditions for water accumulation in the solid reacting mass during SSP, it is reasonable to presume that in the presence of a strong catalyst, as was the herewith studied antioxidant, the significant amount of water produced in the confined amorphous regions finds it difficult to escape because of the hydrophilicity of the organoclay.

In particular, similar effects involving the performance of strong SSP catalysts have been mentioned in the past by Papaspyrides et al.[5–7] It was noted that in the case of very efficient catalysts for the direct polymerization of hydrophilic nylon salts in the solid state, there was a critical polycondensation water amount, above which the catalyst performance was not beneficial for the reaction process and caused the so-called solid–melt transition phenomena. In other words, an inability to remove this high amount of polycondensation water was encountered. This was due to the tendency of this water to be firmly or loosely bound to the hydrophilic sites of the salt. It is challenging to assume that something similar happened herewith, where instead of the
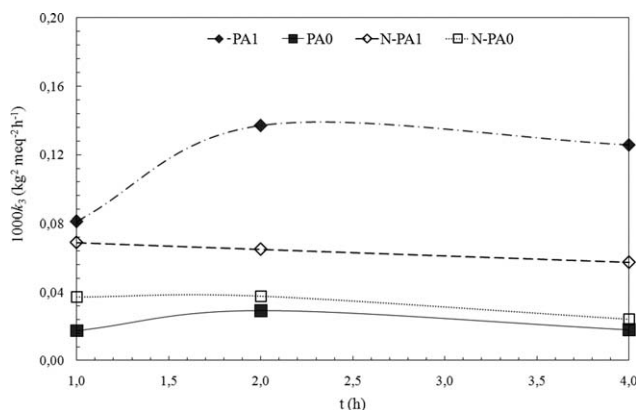

Figure 5 Reaction rate constants ($1000k_3$) versus SSP time at 200°C for the PA0, PA1, N-PA0, and N-PA1 grades.

nylon salt hydrophilic sites, clay's hydrophilicity played the role of the polycondensation water trap. Such a difficulty of the byproduct to escape, in turn, results in the attainment of the reaction equilibrium, especially for long SSP times, when the process becomes diffusion-controlled.[2,3] This assumption can be supported by the evolution of the reaction rate constants as a function of SSP time (Fig. 5): at the early stages of SSP (1 h), the influence of water accumulation in the reacting mass was not dominant; this resulted in similar rate constants for PA1 and N-PA1. As SSP proceeded, larger water amounts were formed, the relevant accumulation in nanocomposites grades prevailed, and the rate constants decreased.

In addition to the aforementioned organoclay hydrophilicity, another feature of these materials that could have also hindered the escape of polycondensation water was their well-known barrier properties.[24,40] At this point, we should mention that in our recent study,[32] such an effect was not found to dominate the SSP reaction rate because a notable catalysis (53% rate increase) in the presence of organoclay was observed, as mentioned in the Introduction. However, in the herewith studied combination of antioxidant and clay, the catalyzing effect was much more intense than in the single clay case (nearly quadruple: a 197% vs 53% rate increase, respectively). This led to the formation of a significantly higher amount of polycondensation water. Therefore, in this case, it was reasonable to assume that the clay barrier action may have played some role in the escape of the condensate because of its higher amount.

Another possible explanation of the observed catalysis counteraction between the antioxidant and organoclay was based on recent literature, which reported the antagonism between antioxidants and clays, with respect to the exploration of nanocomposite systems' inferior oxidation and photooxidation behavior compared to virgin ones.[41–43] More specifically, interactions between the stabilizer and the filler due to adsorption mechanisms were considered to be responsible for this influence. The surface area of the filler and pore volumes, surface functionality, and hydrophilicity, among other factors, have been found to be potential elements of the interaction.[41] In addition, there have been several works reporting the adsorption of phenolic moieties on the clay surface due to the polarity of both species.[44,45] If we combine the previous points, an additional parameter of the counteraction between the antioxidant and organoclay could be the occurrence of adsorption phenomena of the catalyst (phosphite) on the high interfacial area of the clay platelets.

In conclusion, despite the described counteractions, it should be mentioned that the combination of clay and antioxidant was proven to be a strong catalyst system, as it almost tripled the PA 6,6 SSP rate (a 197% increase). This combination yielded a final product of M_n sufficient for further processing, which also bore the advantages of long-term thermal stability because of its antioxidant component and the nanotechnology benefits in terms of material properties. Therefore, the outcome of this work promotes the concept of multifunctional catalyst systems, which accelerate the reaction simultaneously with optimization of the end-product properties.

CONCLUSIONS

In this work, we focused on the catalyzed SSP of PA 6,6, by exploring the catalytic performance of a phosphorous-containing antioxidant and a combination of antioxidant and clay. The antioxidant at 1 phr concentration was found to strongly catalyze the reaction by quintupling the reaction rate; this was attributed to its triphenylphosphite constituent. However, a reduced antioxidant catalytic performance was observed when it was tested in conjunction with clay, and this was ascribed to significant counteractions between them: the clay's hydrophilicity acted as a polycondensation water trap and hindered the escape of the byproduct. The latter effect was also related to the clay's barrier properties, whereas the occurrence of adsorption phenomena on the nanofillers surface was assumed to inhibit the diffusion and, thus, catalytic performance of the antioxidant. Nevertheless, despite the observed counteractions, the antioxidant–clay system was proven to catalyze SSP by tripling the reaction rate. This promoted the concept of multifunctional catalyst systems, which could improve all aspects of the PA 6,6 SSP process by accelerating the reaction, ensuring thermal stability, and simultaneously bearing the nanocomposite advantages in the end-product properties.

References

1. Palmer, R. In Encyclopedia of Polymer Science and Technology; Wiley: Hoboken, NJ, 2002; Vol. 3, p 620.
2. Solid State Polymerization; Papaspyrides, C.; Vouyiouka, S., Eds.; Wiley: Hoboken, NJ, 2009.
3. Vouyiouka, S.; Karakatsani, E.; Papaspyrides, C. Prog Polym Sci 2005, 30, 10.
4. Pfaendner, R. In Solid State Polymerization; Papaspyrides, C.; Vouyiouka, S., Eds.; Wiley: Hoboken, NJ, 2009.
5. Papaspyrides, C.; Kampouris, E. Polymer 1986, 27, 1433.
6. Papaspyrides, C.; Kampouris, E. Polymer 1986, 27, 1437.
7. Katsikopoulos, P.; Papaspyrides, C. J Polym Sci Part A: Polym Chem 1994, 32, 451.
8. Korshak, V.; Frunze, T. Synthetic Heterochain Polyamides; IPST: Jerusalem, 1964; p 120.
9. Gaymans, R. In Polymerization Reactors and Processes; Henderson, J.; Bouton, C., Eds.; ACS Symposium Series 104; American Chemical Society: Washington, DC, 1979.

10. Hiemenz, P. Polymer Chemistry: The Basic Concepts; Marcel Dekker: New York, 1984; p 306.
11. Dujari, R.; Cramer, G.; Marks, D. (to E. I. Du Pont de Nemours and Co.). WIP Pat. WO 98/23666 (1998).
12. Blanchard, E.; Cohen, J.; Iwasyk, J.; Marks, D.; Stouffer, J.; Aslop, A.; Lin, C. (to E. I. Du Pont de Nemours and Co.). WIPO Pat. WO 99/10408 (1999).
13. Pfaendner, R.; Hoffmann, K.; Herbst, H. (to Ciba-Geigy AG). WIPO Pat. WO 96/11978 (1996).
14. Fink, J.; Pfaendner, R.; Papaspyrides, C. D.; Vougiouka S. N. (to Ciba Specialty Chemicals Holding, Inc.). WIPO Pat. WO 2007006647 (2007).
15. Vouyiouka, S. N.; Papaspyrides, C. D.;Pfaendner R. Macromol Mater Eng 2006, 291, 1503.
16. Brignac, E. P.; Duke, B. H.; Nunning, W. J.; Snook R. J. U.S. Pat. 5,116,919 (1992).
17. Katsarava, R. D. Russ Chem Rev 1989, 58, 891.
18. Ogata, N.; Tanaka, H. Polym J 1971, 2, 672.
19. Yamazaki, N.;Higashi F. Tetrahedron 1974, 30, 1323.
20. Yamazaki, N.; Matsumoto, M.; Higashi, G. J Polym Sci Polym Chem Ed 1975, 13, 1373.
21. Aharoni, S. M.; Hammond, W. B.; Szobota, J. S.; Masilamani, D. J Polym Sci Polym Chem Ed 1984, 22, 2567.
22. Aharoni, S. M.; Hammond, W. B.; Szobota, J. S.; Masilamani, D. J Polym Sci Polym Chem Ed 1984, 22, 2579.
23. Aharoni, S. M. Int J Polym Mater 1994, 26, 9.
24. Pavlidou, S.; Papaspyrides, C. D. Prog Polym Sci 2008, 33, 1119.
25. Kiliaris, P.; Papaspyrides, C. D. Prog Polym Sci 2010, 35, 902.
26. Kiliaris, P.; Papaspyrides, C. D.; Pfaendner, R. Macromol Mater Eng 2008, 293, 740.
27. Pfaendner, R.; Papaspyrides, C.; Kiliaris, P. (to BASF SE). WIPO Pat. WO2010069835A1 (2010).
28. Yu, H.; Han, K.; Yu, M. J Appl Polym Sci 2004, 94, 971.
29. Bikiaris, D. N.; Achilias, D. S.; Giliopoulos, D. J.; Karayannidis, G. P. Eur Polym J 2006, 42, 3190.
30. Bikiaris, D. N.; Karavelidis, V.; Karayannidis, G. P. Macromol Rapid Commun 2006, 27, 1199.
31. Achilias, D. S.; Bikiaris, D. N.; Karavelidis, V.; Karayannidis, G. P. Eur Polym J 2008, 44, 3096.
32. Boussia, A. C.; Konstantakopoulou, M. O.; Vouyiouka, S. N.; Papaspyrides, C. D. Macromol Mater Eng 2011, 296, 168.
33. Boussia, A. C.; Vouyiouka, S. N.; Porfyris, A. D.; Papaspyrides, C. D. Macromol Mater Eng 2010, 295, 812.
34. Vouyiouka, S. N.; Papaspyrides, C. D.; Weber, J. N.; Marks, D. N. J Appl Polym Sci 2005, 97, 671.
35. Bacon, K.; Charles, F. In Encyclopedia of Polymer Science and Technology; Mark, H., Bikales, N., Eds.; Interscience: New York, 1966; Vol. 5, p 37.
36. Young, R.; Lovell, P. Introduction to Polymers; Chapman & Hall: London, 1991; pp 176, 195.
37. Boussia, A.; Damianou, C.; Vouyiouka, S.; Papaspyrides, C. J Appl Polym Sci 2010, 116, 3291.
38. Pomerlau, D. G. (to Engineered Drilling Solutions, Inc.). WIPO Pat. WO2007/118328 (2007).
39. Xie, W.; Gao, Z.; Pan, W.-P.; Hunter, D.; Singh, A.; Vaia, R. Chem Mater 2001, 13, 2979.
40. Hatzigrigoriou, N.; Papaspyrides, C. D. J Appl Polym Sci 2011, 126, 3720.
41. Pfaendner, R. Polym Degrad Stab 2010, 95, 369.
42. Morlat-Therias, S.; Mailhot, B.; Gonzalez, D.; Gardette, J.-L. Chem Mater 2005, 17, 1072.
43. Allen, N. S.; Edge, M.; Corrales, T.; Childs, A.; Liauw, C. M.; Catalina, F. L. Polym Degrad Stab 1998, 61, 183.
44. Boyd, S. A.; Shaobai, S.; Lee, J. F.; Mortland, M. Clay Clay Miner 1988, 36, 125.
45. Mortland, M. M.; Shaobai, S.; Boyd, S. A. Clay Clay Miner. 1986, 34, 581.